KURENAI

Kyoto University Research Information Repository

KYOTO UNIVERSITY

Title	Role of Ti Antisitelike Defects in SrTiO3
Author(s)	Choi, Minseok; Oba, Fumiyasu; Tanaka, Isao
Citation	PHYSICAL REVIEW LETTERS (2009), 103(18)
Issue Date	2009-10
URL	http://hdl.handle.net/2433/109873
Right	© 2009 The American Physical Society
Type	Journal Article
Textversion	publisher

Kyoto University

Role of Ti Antisitelike Defects in SrTiO$_3$

Minseok Choi,[1,*] Fumiyasu Oba,[1,†] and Isao Tanaka[1,2]

[1]*Department of Materials Science and Engineering, Kyoto University, Sakyo, Kyoto 606-8501, Japan*
[2]*Nanostructures Research Laboratory, Japan Fine Ceramics Center, Atsuta, Nagoya 456-8587, Japan*

Through first-principles calculations, the role of Ti antisitelike defects in the electrical and optical properties of SrTiO$_3$ is proposed. Significant Ti off-centering from the Sr site toward the [100] or [110] direction leads to switchable polar states, and attractive interactions with the O vacancy drive them to form defect pairs. In these defect configurations, localized electronic states are introduced below the conduction band minimum. Our findings on Ti antisitelike defects suggest that they are responsible for the ferroelectricity and blue light emission in nonstoichiometric SrTiO$_3$.

In recent years, SrTiO$_3$ has been greatly focused on because of its variety of outstanding physical properties: (i) an insulator-metal transition and superconductivity at low temperatures by electron doping [1,2], (ii) the formation of a two-dimensional electron gas at interfaces between SrTiO$_3$ and other oxides [3], (iii) blue light emission in Ar$^+$-irradiated, electron-doped, and O-deficient SrTiO$_3$ [4], and (iv) ferroelectricity without any intentional doping [5]. At present, it is considered that the O vacancy (V_O) is intimately related to these phenomena. The formation of V_O clusters has been suggested through scanning transmission electron microscopy observation [6]. A recent density functional study [7] showed that linear V_O clustering is more stable than isolated V_O and is accompanied by strong electron localization at the neighboring Ti 3d states, which can correspond to a blue light emission level inside the band gap. On the other hand, several experimental studies have revealed the presence of a Sr vacancy (V_{Sr}) and its complexes [8,9]. In spite of the fact that defects other than V_O can also contribute to the above issues, such a possibility has not yet been discussed in depth.

In this Letter, we provide new insight into nonstoichiometric SrTiO$_3$ through a systematic first-principles study of Ti antisitelike defects. Our results demonstrate that off-centered Ti from the Sr site (Ti$_{OC}$), regarded as a *polar* defect pair composed of a Ti interstitial (Ti$_i$) and V_{Sr}, has a low formation energy comparable to that of V_O. Ti$_{OC}$ is switchable between its different configurations, and forms a defect pair with V_O (Ti$_{OC}$ + V_O) as a result of attractive interactions. Such features can explain the observation of ferroelectricity in undoped SrTiO$_3$ [5] as well as the formation of V_{Sr}-related defect species [8,9]. Besides, these defects introduce deep electronic states in the band gap, which can contribute to blue light emission [4] and optical absorption involving two in-gap levels [10,11].

The calculations were performed using the projector augmented-wave (PAW) method [12] and the Perdew-Burke-Ernzerhof generalized gradient approximation (GGA) [13] as implemented in the VASP code [14]. PAW data sets with radial cutoffs of 1.3, 1.3, and 0.8 Å were used for Sr, Ti, and O, respectively. The electronic wave functions were described using a plane wave basis set with an energy cutoff of 400 eV. To correct the on-site Coulomb interaction of the Ti 3d orbitals, a rotationally invariant $+U$ method [15] was applied with $U = 5.0$ eV and $J = 0.64$ eV [7,16]. A $3 \times 3 \times 3$ supercell containing 135 atoms and k points sampled using a $2 \times 2 \times 2$ mesh were used. The atomic coordinates were relaxed until the Hellmann-Feynman force acting on each atom was reduced to less than 0.02 eV/Å.

The defect formation energies are evaluated as

$$E^f(D^q) = E_T(D^q) - E_T(H) - \sum_i n_i \mu_i + q(E_V + E_F),$$

(1)

where $E_T(D^q)$ is the total energy of a supercell with a defect D in charge state q, and $E_T(H)$ is the total energy of a perfect SrTiO$_3$ supercell. n_i is the number of type i atoms added to ($n_i > 0$) and/or removed from ($n_i < 0$) the perfect supercell, and μ_i is the atomic chemical potential. Two different O-poor conditions, i.e., the Sr- and Ti-rich limit ($\mu_{Sr} = \mu_{Sr(bulk)}$, $\mu_{Ti} = \mu_{Ti(bulk)}$, and $\mu_{Sr} + \mu_{Ti} + 3\mu_O = \mu_{SrTiO_3(bulk)}$) and the Ti-rich limit ($\mu_{Ti} = \mu_{Ti(bulk)}$, $\mu_{Ti} + \mu_O = \mu_{TiO(bulk)}$, and $\mu_{Sr} + \mu_{Ti} + 3\mu_O = \mu_{SrTiO_3(bulk)}$), were considered to address defect energetics in reduced SrTiO$_3$. E_V and E_F are the valence band maximum (VBM) and the Fermi level measured from the VBM, respectively.

To correct errors associated with an insufficient description of the band structure by the GGA $+ U$ and the use of finite-sized supercells, a few postprocesses were carried out [17–19]: (i) VBM alignment was applied to charged systems using average potentials. (ii) Band-gap corrections were performed on the basis of defect-induced electronic states. The formation energies of V_O, whose one-electron states follow the upward shift of the conduction band due to the U correction, were extrapolated to an experimental
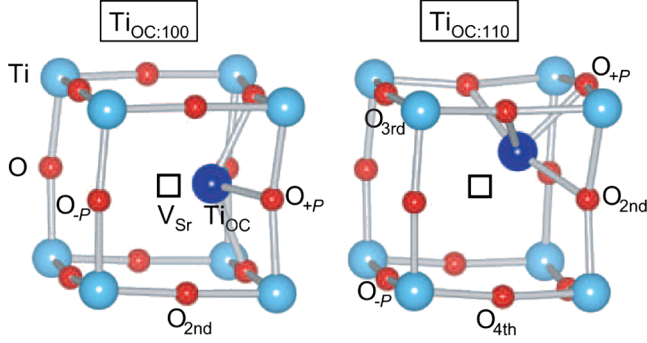
FIG. 1 (color online). Local atomic configurations of off-centered Ti antisitelike defects: $Ti_{OC:100}$ and $Ti_{OC:110}$. O_{+P} and O_{-P} denote O atoms removed as vacancies to form the $[+P]$ and $[-P]$ pairs (see text for details), and O_{2nd}, O_{3rd}, and O_{4th} are the second, third, and fourth nearest-neighboring O atoms of Ti_{OC}, respectively (only one of symmetrically equivalent atoms is indicated for each species).

band gap (E_g^{exp}) of 3.3 eV by adding $m\Delta E_g$, where m and ΔE_g are the number of electrons occupying the defect states and the band-gap difference, equal to $E_g^{exp} - E_g^{GGA+U}$, respectively ($E_g^{GGA+U} = 2.34$ eV). In the case of Ti_{OC} and $Ti_{OC} + V_O$, whose states become deeper from the conduction band minimum (CBM) with increasing U and lie at ~1 eV below the CBM for $U = 5.0$ eV and $J = 0.64$ eV, the formation energies were obtained using the same scheme as for the case of V_O. The validity of this extrapolation scheme for Ti_{OC} and $Ti_{OC} + V_O$ was assessed using the HSE06 hybrid functional [20]. It yields a band gap of 3.25 eV, which is much closer to E_g^{exp} than the GGA + U value. However, the one-electron defect states are located at ~1 eV below the CBM, similar to the case of using GGA + U. This means that the defect states observed in the GGA + U calculations follow the shift of the CBM, and hence our correction scheme for Ti_{OC} and $Ti_{OC} + V_O$ is justified. (iii) The cell-size dependence was examined using supercells containing 40–625 atoms. It is known that the formation energies of V_O in $SrTiO_3$ decrease as the cell size increases owing to atomic relaxation associated with electron delocalization [21]. We found such trends for Ti_{OC} and V_O when the GGA was used. In the GGA + U case, however, the formation energies of Ti_{OC} and neutral V_O are almost independent of the cell size

(they vary within a few tenths of eV). The formation energies of charged V_O decrease as the cell size increases, and the trends with and without the U correction appear to be identical. An extrapolation to the dilute limit, i.e., infinite cell size, indicated that their formation energies can be lowered by ~1 eV from the values for the 135-atom cell that are shown later in Fig. 3. However, this does not alter our discussion and conclusions.

Figure 1 shows the atomic configurations of Ti_{OC}. The Sr site in $SrTiO_3$ is surrounded by 12 symmetrically equivalent O atoms. The antisite Ti atom at this site is unstable, and thereby large Ti off-centering of ~0.8 Å occurs toward one of the six equivalent positions along the [100] direction ($Ti_{OC:100}$) and one of 12 equivalent positions along the [110] direction ($Ti_{OC:110}$) (Fig. 1 and Table I). $Ti_{OC:100}$ forms four Ti–O bonds of length 2.25 Å, and $Ti_{OC:110}$ has one Ti–O bond of length 2.19 Å and four bonds of length 2.33 Å. Such off-centering can be understood in terms of the large difference in ionic radius between Ti^{2+} (0.86 Å) and Sr^{2+} (1.44 Å) [22], similar to the Li off-centering in $K_{0.5}Li_{0.5}NbO_3$ [23]. The distance between the Ti atoms in the $Ti_{OC:100}$ and $Ti_{OC:110}$ configurations is 0.59 Å, and the energy barriers are 0.23 eV for $Ti_{OC:100} \rightarrow Ti_{OC:110}$ and 0.14 eV for $Ti_{OC:100} \leftarrow Ti_{OC:110}$. These values are much smaller than the reported migration energies of 0.6 eV for V_O [7] and 1.2 eV for the linear V_O-cluster [7]. The switching of $Ti_{OC:100} \leftrightarrow Ti_{OC:110}$ is thus very likely. Owing to the large Ti displacements, each Ti_{OC} can also be regarded as a *polar* defect pair, i.e., $Ti_i + V_{Sr}$, having a dipole moment $(+p)$ in the V_{Sr} to Ti_i direction. The $+p$ direction is [100] for $Ti_{OC:100}$ and [110] for $Ti_{OC:110}$. These atomic structures of $Ti_{OC:100}$ and $Ti_{OC:110}$, i.e., $Ti_i + V_{Sr}$, are consistent with the experimental observations of V_{Sr} and related defects [8,9].

Moving on to the electronic structure, both configurations of Ti_{OC} introduce localized states below the CBM in the majority spin component, as shown in Fig. 2 and Table I. No in-gap states are found in the minority spin component, yielding a magnetic moment of $2\mu_B$. However, Ti_{OC} does not have a strong effect on the host conduction and valence bands. In the case of $Ti_{OC:100}$, two deep localized states are located at 0.96 and 1.29 eV below the CBM and have orbital characteristics of d_{yz} and $(d_{3z^2-r^2}$ and $d_{x^2-y^2})$, respectively. $Ti_{OC:110}$ behaves similarly. Its induced states lie 1.02 eV with $(d_{yz}$ and $d_{zx})$

TABLE I. Properties of off-centered Ti antisitelike defects (Ti_{OC}) and pairs of Ti_{OC} with V_O ($Ti_{OC} + V_O$). d denotes the atomic distance from Ti to V_{Sr} in Ti_{OC} and from Ti to V_O in $Ti_{OC} + V_O$. ϵ is the energy of the defect-induced one-electron state measured from the CBM. E^b is the binding energy between Ti_{OC} and V_O.

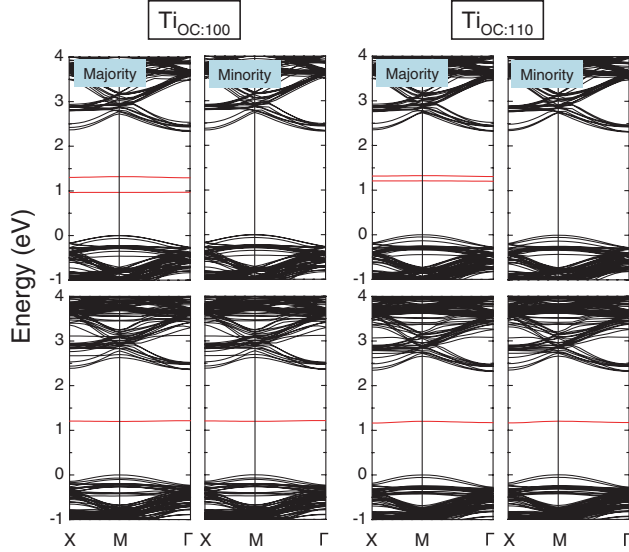| | Ti_{OC} | | $Ti_{OC} + V_O$ [+P] | | | $Ti_{OC} + V_O$ [−P] | | |
	d (Å)	ϵ (eV)	d (Å)	E^b (eV)	ϵ (eV)	d (Å)	E^b (eV)	ϵ (eV)
[100]	0.77	0.96, 1.29	1.80	−0.18	1.10	3.10	+0.01	0.31, 2.12
[110]	0.76	1.02, 1.12	2.25	−0.28	1.15	3.61	−0.10	0.92, 1.11

FIG. 2 (color online). Band structures of neutral Ti_{OC} (upper) and 2+ charged $Ti_{OC} + V_O$ (lower). Each localized in-gap state is occupied by one electron. The VBM is set to zero.

characteristics and 1.12 eV with ($d_{3z^2-r^2}$ and d_{xy}) characteristics below the CBM. Thermodynamical transition levels, $\varepsilon(2+/+)$ and $\varepsilon(+/0)$, occur at 1.54 and 0.31 eV below the CBM for $Ti_{OC:100}$ and 1.17 and 0.24 eV for $Ti_{OC:110}$, respectively [Fig. 3]. Therefore, neither $Ti_{OC:100}$ nor $Ti_{OC:110}$ release their electrons into the conduction band at room temperature; i.e., they are deep donors. Owing to the high formation energies, the concentrations of both defects should be low in the n-type region, i.e., when E_F is close to the CBM, under Sr- and Ti-rich conditions. At the Ti-rich limit, the formation energies of these defects are lowered by ~2 eV, and are comparable to that of V_O in the n-type region. Thus, $Ti_{OC:100}$ and $Ti_{OC:110}$ can be dominant defects in Ti-rich $SrTiO_3$ as well as V_O. It is
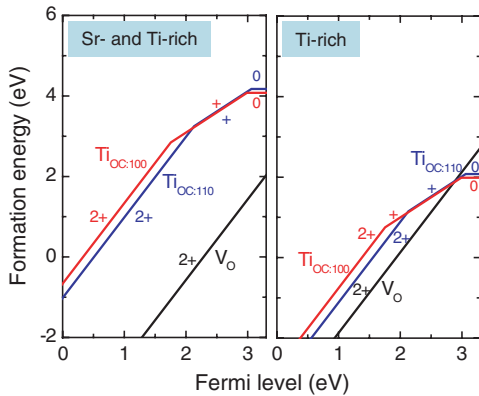

FIG. 3 (color online). Formation energies of Ti_{OC} and V_O as a function of the Fermi level at the Sr- and Ti-rich (left) and Ti-rich (right) limits. The slope corresponds to the charge state, as indicated in the figure. The Fermi level at which the slope changes is denoted as the thermodynamical transition level.

noteworthy that their formation energies are much higher under Sr-poor, Ti-rich, and O-rich conditions; for example, at the limit given as $\mu_{Ti} + 2\mu_O = \mu_{TiO_2(bulk)}$, $\mu_O = \frac{1}{2}\mu_{O_2(molecule)}$, and $\mu_{Sr} + \mu_{Ti} + 3\mu_O = \mu_{SrTiO_3(bulk)}$, they are 4.88 eV higher than the values at the Ti-rich limit. Therefore, Ti_{OC} is unlikely to form under the O-rich conditions.

Another finding for Ti_{OC} defects is that they favor coupling with V_O. In the n-type region, where the neutral and 2+ charge states are energetically the most favorable for Ti_{OC} and V_O, respectively, the binding energy E^b is obtained as

$$E^b = E^f\left((Ti_{OC} + V_O)^{2+}\right) - E^f(Ti_{OC}^0) - E^f(V_O^{2+}). \quad (2)$$

A negative E^b indicates that Ti_{OC} and V_O are preferentially located close to each other (*exothermic*), whereas a positive value means that they repel each other (*endothermic*). By taking into account the two types of V_O locations using an idea in Ref. [24] as an analogy, the stability of the defect pairs is monitored: one binds with the nearest-neighboring V_O lying in (nearly) the same direction as the $+p$ direction, and the other binds with the closest V_O located in (nearly) the opposite direction. The former and latter defect pairs are denoted as $[+P]$ and $[-P]$, and the corresponding O atoms are indicated as O_{+P} and O_{-P} in Fig. 1, respectively. Because of the positive charge of V_O, it is expected that $[+P]$ enhances the $+p$ of isolated Ti_{OC} but $[-P]$ makes it weaker. We found that $[+P]$ is *exothermic* for both $Ti_{OC:100}$ and $Ti_{OC:110}$ and more stable than $[-P]$ by ~0.2 eV [Table I]. Accordingly, we can conjecture that as the V_O concentration increases, the *attractive* interactions facilitate the formation of $Ti_{OC} + V_O$ $[+P]$. $Ti_{OC:100} + V_O$ $[+P]$ and $Ti_{OC:110} + V_O$ $[+P]$ also yield deep localized one-electron states at nearly 1.1 eV from the CBM in both spin components (zero μ_B) [Fig. 2 and Table I]. Spin-polarized configurations with a magnetic moment of $2\mu_B$ are found to be less stable by 0.04 eV for both $Ti_{OC} + V_O$ [25].

On the basis of our results, we now explain two interesting phenomena observed in various experiments, for which the mechanisms are not yet clear. First, how Ti_{OC} and its pair are related to the blue light emission [4] and the two in-gap optical absorption levels [10,11] is clarified. According to the Franck-Condon principle, vertical transition energies have been evaluated as the differences of total energies after the band-gap corrections. The emission energy in the recombination process of an electron (e^-) at the deep donor states of Ti_{OC}^0 with a hole (h^+) at the VBM, i.e., $Ti_{OC}^0 + h^+ \rightarrow Ti_{OC}^+$, is computed to be ~2.3 eV for both $Ti_{OC:100}$ and $Ti_{OC:110}$. The $[+P]$ pairs provide similar energies of ~2.4 eV by $(Ti_{OC} + V_O)^{2+} + h^+ \rightarrow (Ti_{OC} + V_O)^{3+}$. These values are close to the blue light emission energy of ~2.8 eV [4]. For the absorption, when the electrons at the deep states of $Ti_{OC:100}^0$ and $Ti_{OC:110}^0$ are photoexcited to the CBM, they produce absorption ener-

gies of 1.0–1.1 eV for $Ti_{OC}^{0} \rightarrow Ti_{OC}^{+} + e^{-}$ and 1.8–2.1 eV for $Ti_{OC}^{+} \rightarrow Ti_{OC}^{2+} + e^{-}$. Likewise, the $[+P]$ pairs provide energies of ~ 1.0 eV for $(Ti_{OC} + V_{O})^{2+} \rightarrow (Ti_{OC} + V_{O})^{3+} + e^{-}$ and 2.2–2.3 eV for $(Ti_{OC} + V_{O})^{3+} \rightarrow (Ti_{OC} + V_{O})^{4+} + e^{-}$. These transitions are consistent with measurement of the two broad peaks centered at approximately 1.3–1.4 and 2.4–2.5 eV in the absorption spectra [10,11].

Next, the ferroelectricity in the reduced $SrTiO_3$ samples [5] can be explained by Ti_{OC} and $Ti_{OC} + V_{O}$. There are two scenarios considered: (i) Similar to typical displacive-type ferroelectrics, Ti_{OC} has switchable dipole moments, i.e., $Ti_{OC:100} \leftrightarrow Ti_{OC:\bar{1}00}$ (e.g., via $Ti_{OC:110}$, $Ti_{OC:010}$, and $Ti_{OC:\bar{1}10}$) or $Ti_{OC:110} \leftrightarrow Ti_{OC:\bar{1}\bar{1}0}$ (e.g., via $Ti_{OC:010}$, $Ti_{OC:\bar{1}10}$, and $Ti_{OC:\bar{1}00}$), over the low energy barriers of ~ 0.2 eV as described above. The switching energy is comparable to the double-well barriers of ~ 0.1 eV in ferroelectric $PbTiO_3$ [26] and ~ 0.15 eV in $K_{0.5}Li_{0.5}NbO_3$ [23]. With increasing Ti_{OC} concentrations, i.e., decreasing distances between the Ti_{OC}, the long-range dipole-dipole interaction may become stronger and yield a net polarization by the alignment of $+p$ dipole moments. (ii) Recently, ferroelectricity in A-site-doped $SrTiO_3$ has been suggested to be closely connected to the formation of polar nanoregions (PNRs) [27,28], which are known to play a crucial role in ferroelectric relaxor behavior [29]. In Ca- and Pr-doped systems, the PNRs are created around the A-site dopants. By the analogy with the *extrinsic A*-site dopants, it is natural to consider Ti_{OC} as an *intrinsic A*-site dopant. Ti_{OC} and $Ti_{OC} + V_{O}$ in reduced $SrTiO_3$ are expected to create the PNRs around themselves.

The larger experimental net polarization observed in reduced $SrTiO_3$ [5] than that in Ca-doped $SrTiO_3$ is probably due to the large Ti off-centering (~ 0.8 Å) from the Sr site in the Ti_{OC} configurations, which may induce a larger local dipole moment and/or create stronger PNRs compared with those developed by relatively weak Ca off-centering (~ 0.1–0.3 Å) [30].

In conclusion, the crucial roles of the Ti off-centering defects in reduced $SrTiO_3$ are illustrated through first-principles calculations. The Ti off-centering exhibits two stable configurations, switching between them, and coupling with the O vacancy. These defects can lead to the ferroelectric state without intentional doping. Both Ti off-centering configurations and their pairs with the O vacancy produce in-gap energy states, which elucidates the blue light emission and the optical absorption involving two deep levels.

*minseok.choi@ks2.ecs.kyoto-u.ac.jp
†oba@cms.mtl.kyoto-u.ac.jp

[1] J. F. Schooley, W. R. Hosler, and M. L. Cohen, Phys. Rev. Lett. **12**, 474 (1964).

[2] H. Suzuki *et al.*, J. Phys. Soc. Jpn. **65**, 1529 (1996).

[3] A. Ohtomo and H. Y. Hwang, Nature (London) **427**, 423 (2004).

[4] D. Kan *et al.*, Nature Mater. **4**, 816 (2005); D. Kan *et al.*, Appl. Phys. Lett. **88**, 191916 (2006); D. Kan *et al.*, Jpn. J. Appl. Phys. **46**, L471 (2007).

[5] Y. S. Kim *et al.*, Appl. Phys. Lett. **91**, 042908 (2007).

[6] D. A. Muller *et al.*, Nature (London) **430**, 657 (2004).

[7] D. D. Cuong *et al.*, Phys. Rev. Lett. **98**, 115503 (2007).

[8] X. Wang *et al.*, J. Vac. Sci. Technol. A **17**, 564 (1999).

[9] R. A. Mackie *et al.*, Phys. Rev. B **79**, 014102 (2009).

[10] D. Millers *et al.*, Nucl. Instrum. Methods Phys. Res., Sect. B **194**, 469 (2002).

[11] Y. S. Kim *et al.*, Appl. Phys. Lett. **94**, 202906 (2009).

[12] P. E. Blöchl, Phys. Rev. B **50**, 17 953 (1994).

[13] J. P. Perdew, K. Burke, and M. Ernzerhof, Phys. Rev. Lett. **77**, 3865 (1996).

[14] G. Kresse and J. Hafner, Phys. Rev. B **48**, 13 115 (1993); G. Kresse and J. Furthmüller, *ibid.* **54**, 11 169 (1996); G. Kresse and D. Joubert, *ibid.* **59**, 1758 (1999).

[15] A. I. Liechtenstein, V. I. Anisimov, and J. Zaanen, Phys. Rev. B **52**, R5467 (1995).

[16] S. Okamoto, A. J. Millis, and N. A. Spaldin, Phys. Rev. Lett. **97**, 056802 (2006).

[17] F. Oba *et al.*, Phys. Rev. B **77**, 245202 (2008).

[18] M. Choi, F. Oba, and I. Tanaka, Phys. Rev. B **78**, 014115 (2008).

[19] S. Lany and A. Zunger, Phys. Rev. B **78**, 235104 (2008).

[20] A. V. Krukau *et al.*, J. Chem. Phys. **125**, 224106 (2006).

[21] J. P. Buban, H. Iddir, and S. Öğüt, Phys. Rev. B **69**, 180102 (2004).

[22] R. D. Shannon, Acta Crystallogr. Sect. A **32**, 751 (1976).

[23] D. I. Bilc and D. J. Singh, Phys. Rev. Lett. **96**, 147602 (2006).

[24] S. Pöykkö and D. J. Chadi, Phys. Rev. Lett. **83**, 1231 (1999).

[25] We found that the stability of $Ti_{OC:100} + V_{O}$ sensitively depends on spin configurations and applied U values. In the non-spin-polarized case, $[+P]$ is the most stable among $Ti_{OC:100} + V_{O}$ involving V_{O} at various O sites [Fig. 1], while the spin-polarized configuration of $Ti_{OC:100} + V_{O_{2nd}}$ with $2\mu_{B}$ shows a 0.08 eV lower energy than $[+P]$. In contrast, another $U - J$ value of 2.3 eV [7] predicts that $[+P]$ is the most favorable irrespective of the spin configurations. Although these results imply an uncertainty in the most stable configuration and hence the direction of the dipole moment for $Ti_{OC:100} + V_{O}$, we focus on the $[+P]$ and $[-P]$ configurations for concise discussion.

[26] R. E. Cohen, Nature (London) **358**, 136 (1992).

[27] U. Bianchi *et al.*, Phys. Rev. B **51**, 8737 (1995).

[28] R. Ranjan *et al.*, Phys. Rev. B **76**, 224109 (2007).

[29] I.-K. Jeong *et al.*, Phys. Rev. Lett. **94**, 147602 (2005).

[30] G. Geneste and J.-M. Kiat, Phys. Rev. B **77**, 174101 (2008).